Structural, morphological and luminescence properties of hexagonal ZnO particles synthesized using wet chemical process

FB Dejene[1*], L. Koao[1], JJ Dolo[1] and HC Swart[2]

[1]Department of Physics, University of the Free State (QwaQwa campus, Private Bag X13, Phuthaditjhaba, 9866, South Africa)
[2]Department of Physics, University of the Free State, P.O. Box 339, Bloemfontein, 3057, South Africa.

[*]Corresponding author. Tel: +27587185263, fax: +275871853444,
e-mail adress: dejenebf@qwa.ufs.ac.za

Abstract
ZnO particles of different sizes were synthesized using a simple wet chemical method. This is a very attractive method, inexpensive and convenient for large area deposition. It is a low temperature process and the properties are easy to change by varying the deposition parameters. So-prepared ZnO particles were then characterized using scanning electron microscope, X-ray diffraction, PL spectroscopy and UV-Vis optical absorption spectra. The XRD pattern of a typical ZnO structures grown using wet-chemical process exhibit sharp diffraction peaks characteristic of the ZnO wurtzite hexagonal phase (wurtzite-type, space group P63mc, JCPDS card file No. 36-1451). SEM image confirm the hexagonal ZnO structure. The UV-vis absorption spectra of ZnO structures show that samples prepared at high pH value demonstrated similar properties as bulk materials. It was also found that energy band gap (Eg) does not increase significantly with the increase in molar concentration of reactant solution. The PL measurement depicts that the relative intensity difference between UV emission and green emission in ZnO generally depends on the process condition, particle size, source materials, and synthesis method. The characteristic emissions were found to be extremely broad and this broadening may be due to photon assisted by phonon transition.

1. Introduction

Zinc oxide (ZnO) nanostructures are semiconductor materials with a wide direct band gap of 3.37 eV, a large exciton binding energy (60 meV) and excellent chemical stability. It is well known that the properties of zinc oxide depend on both size and morphology of the particles. Nanostructured ZnO exhibits numerous characteristics that may enable it for various applications, such as gas sensors [1], biosensors [2], solar cells [3], varistors [4], photo detectors [5] and photo catalysts [6]. Different methods have been developed to prepare nanostructured ZnO, including sol-gel [7], spray pyrolysis [8], electrodeposition [9], microwave-assisted techniques [10], chemical vapor deposition [11], hydrothermal [12] and precipitation methods [13]. Most of the reported experimental methods cannot be extensively applied on a large scale. Among these, chemical bath deposition (CBD) method has achieved great attention due to simplicity and cost effective. The aim of this work is to study the optical transmittance, the morphological and structural properties of the ZnO powders as prepared by CBD method using zinc acetate and thiourea as precursors. Thiourea is an organic compound of carbon, nitrogen, sulfur, and hydrogen. It is a versatile reagent in organic synthesis. It can be an interesting inorganic matrix modifier due to its large dipole and ability to form an extensive hydrogen bond network.

2. Experimental procedure

The ZnO microstructures were prepared by using cheap, scalable and versatile chemical deposition process (CBD). The precursors used during deposition process are zinc acetate, holding thiourea and ammonia constant. The growth conditions such as concentrations, pH, depositions time and synthesis temperature were optimized to obtain highly crystalline ZnO structure with optimum optical properties.
After the precipitates were formed, the precipitates were filtered and washed with ethanol. The obtained powders were dried at ambient conditions for several days. After that the powders were ready to be characterized. The particle size, morphology , structural and luminescent properties of the as-synthesized phosphors were examined by means of scanning electron microscopy (SEM), X-ray diffraction (XRD), Uv-vis spectroscopy and Photoluminescence (PL).

3. Results

3.1 Morphological and structural properties

Representative SEM images of as prepared ZnO at various pH are shown in Fig. 1. Low-magnification SEM image (Fig. 1(a)) show that the wurtzite structure ZnO are formed. In a high-magnification image (Fig. 1(b)), it can be seen that the as-prepared ZnO particles are various in size. On a whole, these ZnO particles sizes range from sub microns to few microns in edge lengths.

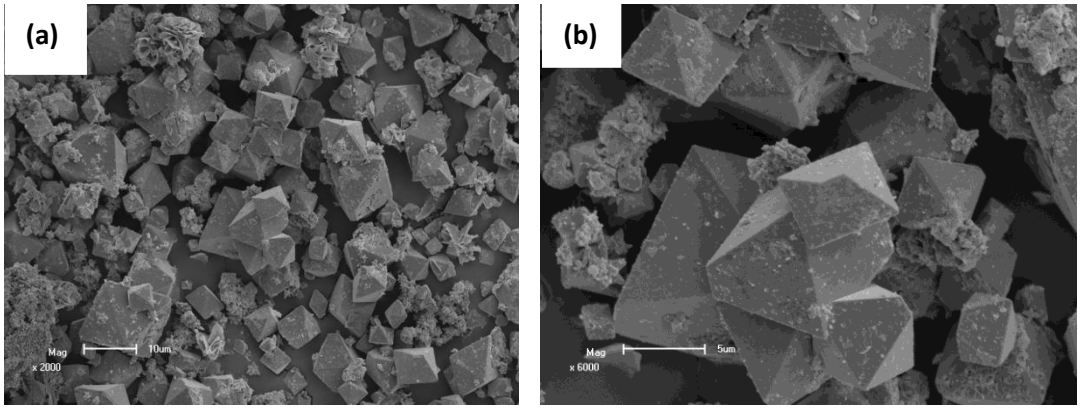

Figure 1: SEM images for the as-formed various sized ZnO:Ce $^{3+}$ particles: (a) image with low magnification and (b) high magnification

Fig. 2 (a) present's representative XRD pattern of a typical ZnO particle structures grown using wet-chemical process. It exhibit sharp diffraction peaks characteristic of the ZnO wurtzite hexagonal phase (wurtzite-type, space group P63mc, JCPDS card file No. 36-1451), which implies that pure ZnO was formed. The sharp and intense peaks in the XRD spectrum indicate well crystalline of pure ZnO. No significant impurities or characteristic diffraction peaks from other phases were detected. Energy dispersive X-ray analysis (EDX) indicated the presence of zinc and oxygen for all the as prepared samples (Fig. 2(b)). The average atomic ratio of O/Zn, calculated from the quantification of the peaks, gives the value of 0.51, 0.56, 0.57 and 0.58 for different pH values of the precursors at pH of 5.6, 6.8, 8.8 and 9, respectively. These results indicate that the average atomic ratio of O/Zn increases with increasing pH, ratios of the particles are slightly lower than the stoichiometric ratio (O/Zn = 1) and the surface of the samples is rich in metal.

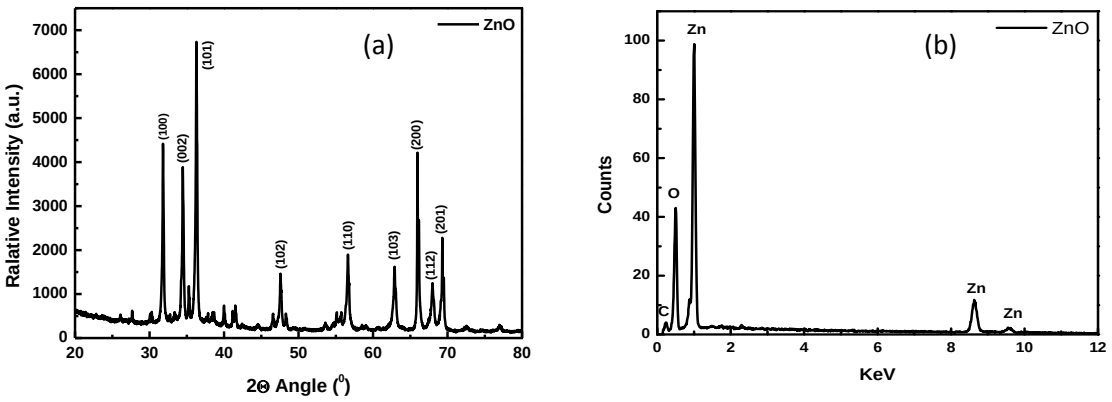

Figure 2: (a) A representative XRD pattern for the ZnO samples prepare at different pH and (b) the EDX pattern of the ZnO deposited by CBD method at 80 ^{o}C.

Deviation from the atomic percentages of O/Zn ratios could be attributed to the presence of atomic percentage of sulfur from thiourea as revealed from the EDX of the particles. In our chemical bath deposition experiment, the pH is maintained at alkaline condition and hence there is a significant influence of OH_ ions on the deposition process, which favors the inclusion of oxygen in the ZnO particles, resulting in amount of oxygen in cooperated [14]. The excess of Zn is bounded to sulfur in the form of ZnS.

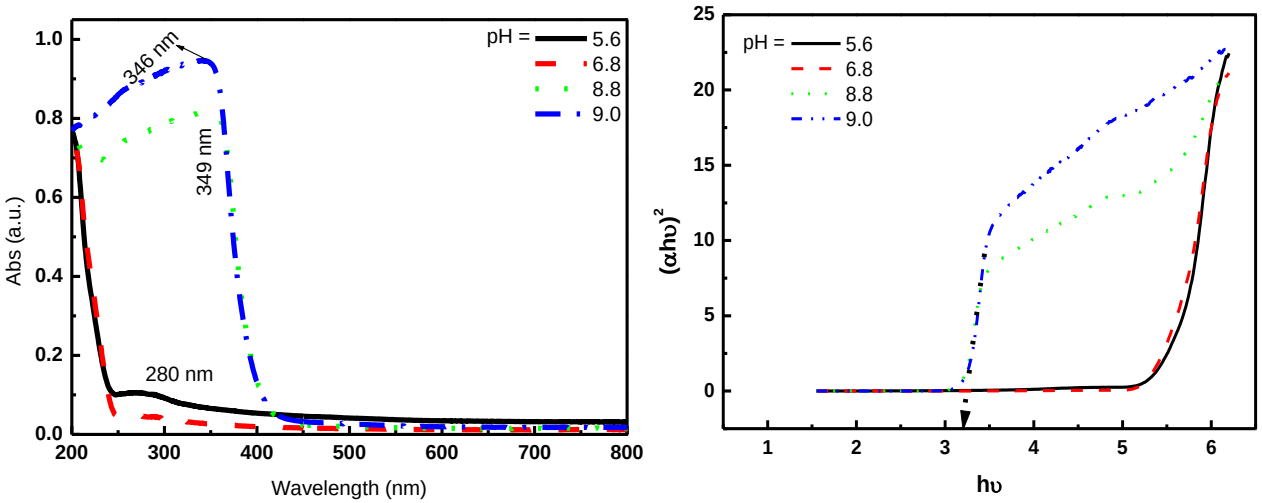

Figure 3: (a) Optical absorption spectra and (b) calculated band gap energy of ZnO particles synthesized at different pH.

3.2 Optical properties

The UV-vis absorption spectra of ZnO structures synthesized at various pH is shown in Fig. 3, which exhibit a strong absorption edge in the near-IR region. Samples prepared at high pH value demonstrated similar properties as bulk materials while those prepared at low pH does not show ZnO absorption

properties. The absorption coefficient (α) was analyzed using the following expression for near-edge optical absorption of semiconductors:

$$\alpha h\nu = K(h\nu - E_g)^2$$

where K is constant, Eg is the separation between the valance and conduction bands. The band gap values were determined from the intercept of the straight-line portion of the $(\alpha h\nu)^2$ against the $h\nu$ graph on the $h\nu$-axis using fitting program. The band-gap value was calculated to be approximately 3.2 eV. The band-gap values are similar to that of bulk value of wurtzie ZnO. The electronic level diagram of ZnO and corresponding possible visible emissions are shown in Figure 4. The visible emissions are mainly classified into green, orange, and red emissions. Vanheusden et. al. [15] suggested a correlation between green luminescence and singly ionized oxygen vacancies in reduced ZnO. According to them, green emission results from the recombination of a photo generated hole with the singly ionized charge state of oxygen vacancy. Dijken *et al.* [16] suggested that green emission results from the recombination of a conduction band electron with a doubly ionized oxygen vacancy (V_o^{++}) centers. This recombination centers can be created when a singly ionized oxygen vacancy traps a hole. Thus, green emission is also associated with the singly ionized oxygen vacancy in this case. Bylander [17] suggested a model in which the green luminescence arises from an electronic transition from zinc interstitial to a Zn vacancy. Egelhaaf *et al.* [18] proposed model related with a transition from a donor to an acceptor center. The donor and acceptor are assumed to be a singly ionized oxygen vacancy ($V_o^{\cdot}$) and zinc vacancy ($V_{zn}^{''}$), respectively. The green emission arises from this donor to acceptor transition mechanism in this case. In polycrystalline materials and in powders, band bending will occur at grain boundaries and free surfaces. Band bending creates an electron depletion region of width (W) at the particle surfaces. In the fraction of this region where the Fermi level (E_f) locates below the energy level, all oxygen vacancies will be in the diamagnetic state.

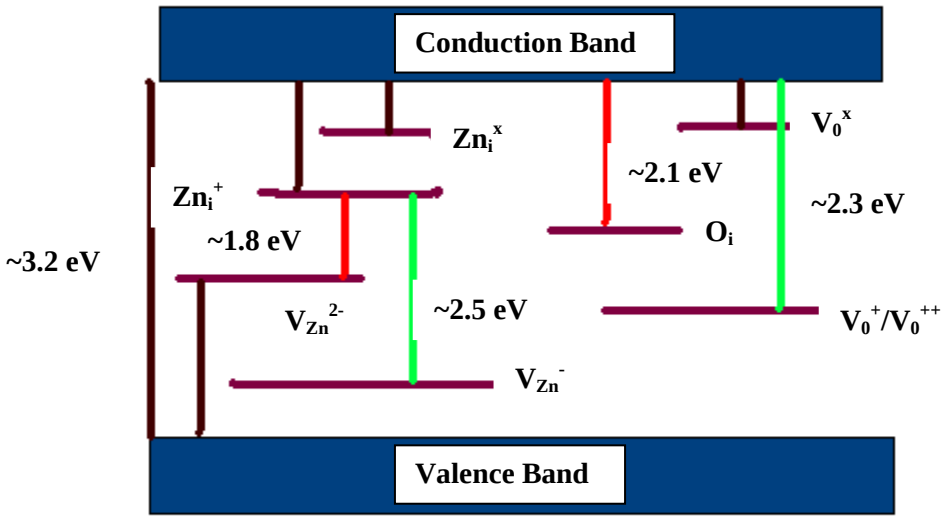

Figure 4: Schematic electronic level of ZnO. The arrows indicate possible non-radiative or radiative transition.

The width of the depletion region and the fraction of diamagnetic are inversely proportional to the free carrier concentration in the particle. If the green luminescence is associated with the singly ionized oxygen vacancy, no green emission will occur in the depleted region of the grain that only contains $V_o^{\cdot\cdot}$. Thus, the width of depletion region and free carrier concentration play an important role to generate green emission in nano-structured ZnO. PL measurements were done at room temperature. PL emission spectrum of ZnO particles exhibits a UV emission band located at around 340 nm and a broad green emission band peaking at around 480 nm. UV emission intensity is mainly dependent on the crystallinity of the ZnO structures, which means that wurtzite ZnO have a higher degree of crystalline ZnO particles. The relative intensity difference between UV emission and green emission in ZnO generally depends on the process condition, particle size, source materials, and synthesis method. The characteristic emissions were found to be extremely broad and this broadening may be due to photon assisted by phonon transition. From the different sample preparation a clear contrast in luminescence property has been observed which we are reporting. It is concluded that synthesis of ZnO with theourea, luminescence intensity was observed to significantly depend on the pH and the amount of Ce concentrations.

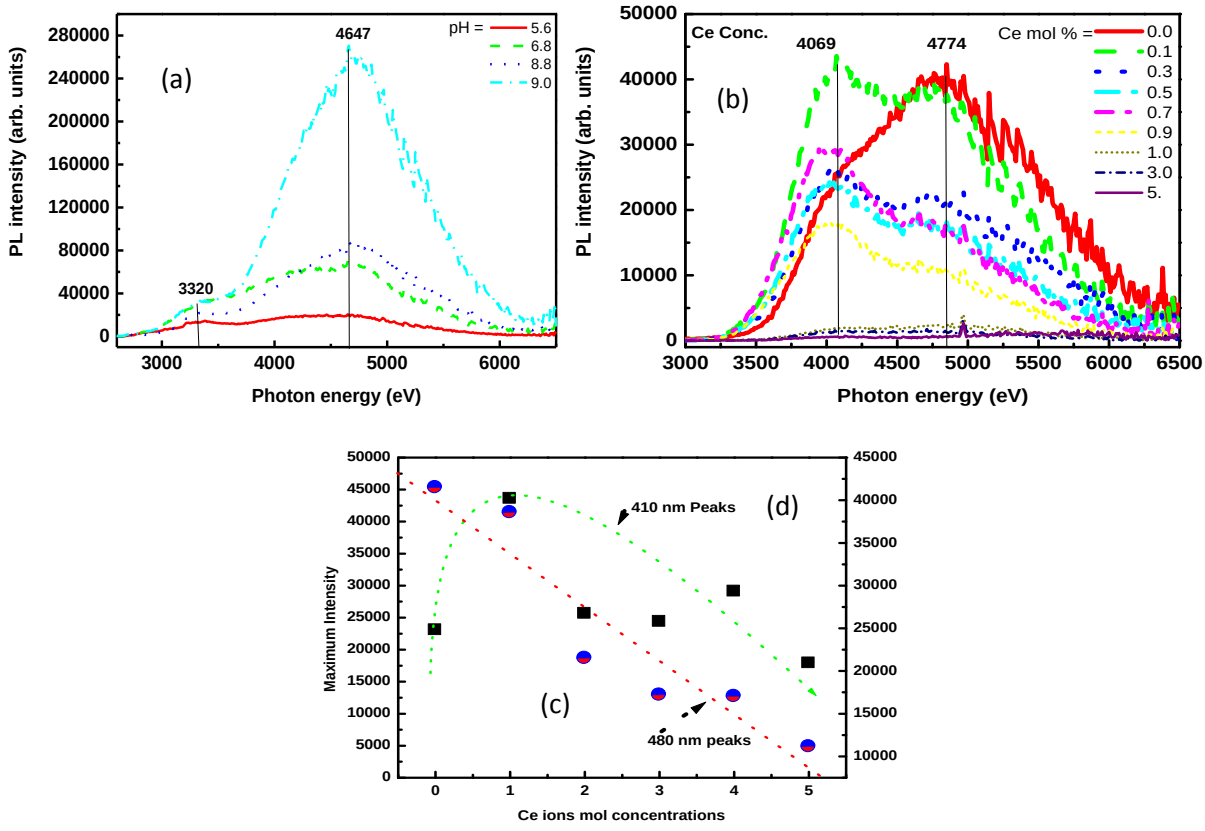

Figure 5: PL emission spectra of nanosized ZnO particles (a) at various pH and (b) Ce concentrations. (c) Normalized maximum visible emission intensities. d) Maximum visible emission peak position.

The higher green emission intensity relative to UV emission intensity implies that the main intrinsic defect in ZnO particles is a singly ionized oxygen vacancy and its trapping efficiency for radiative recombination is much higher than that of UV emission. In addition, the higher green emission efficiency of ZnO particles might be associated with the higher density of $V_o^*$and less depletion region width. The

comparisons of PL emission spectra between as-grown ZnO particles are shown in Figure 4 (a) and (b). No significant change in the UV emission was observed with variation of the precursor pH but the green emission of ZnO particles rapidly increases with pH increase. The addition of Ce ions slightly enhanced the green emission at low concentrations and quenches the luminescence at concentration above 1% due concentration quenching. The enhancement might be attributed to the less surface trapping rate of exited charge carriers and less depletion region width near the surface of ZnO. Thus, the presence of Ce ions enhances the PL emission of ZnO by decreasing the number of surface traps and increasing the available density responsible for green luminescence in ZnO. The UV emission disappeared due to the presence of Ce ions.

4. Conclusions

Highly crystalline ZnO particles were synthesized by CBD method. The X-ray diffraction analysis showed that film is polycrystalline in nature. The particles have a direct band gap with an optical value of 3.2 eV which is in good agreement with the standard value. The Pl measurements show higher green emission intensity as compared to UV emission intensity. The optical characterization shows, all the powders exhibit low absorbance (high transmittance) in the visible region. This makes the powders suitable for use as an antireflection coating for hetero-junction solar cells and optoelectronic applications.

Acknowledgement

The financial support of the National Research Foundation (NRF) and the University of Free State are acknowledged.

References

[1]. Cheng X L, Zhao H, Huo, L H, Gao S and Zhao J G ZnO 2004 *Sens Actuators*, **102** 248–252.
[2]. Topoglidis E, Gass A E-G, Oregan B and Durrant J R 2001 *J. Electroanal. Chem.*, **517** 20–27.
[3]. Hames Y, Alpaslan Z, K¨osemen A, San S E and Yerli Y 2010 *Solar Energy*, **84** 426–431.
[4]. Wu J, Xie C S, Bai Z K, Zhu B L, Huang K J, Wu R 2002 *Mater. Sci. Eng.*, **95** 157–161.
[5]. Sharma, P.; Sreenivas K, Rao K V 2003 *J. Appl. Phys.*, **93** 3963–3970.
[6]. Kamat V P, Huehn R and Nicolasecu R 2002 *J. Phys. Chem.*, **106** 788–794.
[7]. Takumoto M S, Pulcinelli S H, Santilli C V, Briois V 2003 *J. Phys. Chem.*, **107** 568–574.
[8]. Okuyama K and Lenggoro I W 2003 *Chem. Eng. Sci.*, **58** 537–547.
[9]. Bayandori-Moghadam A, Nazari T, Badraghi J and Kazemzadeh M 2009 *Int. J. Electrochem.*, **4** 247–257.
[10]. Hu X L, Zhu YJ and Wang S W 2004 *Mater. Chem. Phys.*, **88** 421–426.
[11]. Wu J J and Liu S C 2002 *Adv. Mater.*, **14** 215–218.
[12]. Zhai H J, Wu W H, Lu F and Wang H S 2008 *Mater. Chem. Phys.*, **112** 1024–1028.
[13]. Bitenc M, Marinsek M and Crnjak-Orel Z 2008 *J. Eur. Ceram. Soc*, **28** 2915–2921.
[14]. Nasr T B, Kamoun N and Guasch C Mater., 2006 *Chem. Phys.*, **96** 84.
[15]. Vanheusden K, Warren W L, Seager C H, Tallant D R and Voigt J A 2006 *J.Appl. Phys.*, **79**, 7983.
[16]. van Dijken A, Meulenkamp E A, Vanmaekelbergh D and Meijerink A 2000 *J.Phys. Chem. B*, **104**, 1715.
[17]. Bylander E G 1978 *J. Appl. Phys.*, **49** 1188.
[18]. Egelhaaf H –J and Oelkrug D , 1996 *J. Cryst. Growth*, **161**, 190.